Contribution from the Department of Chemistry, The Pennsylvania State University, University Park, Pennsylvania 16802, and The Contrast Media Research Department, Squibb Institute for Medical Research, P.O. Box 191, New Brunswick, New Jersey 08903

Spectroscopic Characterization of the Europium(III) Complexes of a Series of *N,N'*-Bis(carboxymethyl) Macrocyclic Ether Bis(lactones)

Richard C. Holz,[†] C. Allen Chang,[‡] and William DeW. Horrocks, Jr.*[,†]

Received July 31, 1990

The Eu^{3+} and Y^{3+} complexes of a series of *N,N'*-bis(carboxymethyl) macrocyclic ether bis(lactone) ligands derived from ethylenediaminetetraacetic acid (EDTA) were characterized in solution by using Eu^{3+} laser-induced luminescence and ^1H and ^{13}C NMR spectroscopy. The complexation of EDTA was also studied for comparison purposes. These ligands form 1:1 complexes with Eu^{3+} at the concentrations studied (10 μM), with the luminescence lifetimes in H_2O and D_2O providing the number of coordinated water molecules. The $^7F_0 \rightarrow {}^5D_0$ excitation spectra indicate that for each of the complexes two isomers are present in fast exchange on the $^5D_0$ time scale. The spectra obtained for the macrocyclic complexes are identical with that of $[EuEDTA]^-$, suggesting that the ether moieties of the macrocyclic ligands are not involved in direct coordination to the metal ion. These results are corroborated by the ^1H and ^{13}C NMR spectra of the Y^{3+} complexes. Changes in the coordination environment of the Eu^{3+} ion as a function of pH and temperature were observed for each complex. These results suggest that two species, which involve different numbers of coordinated carboxylate moieties, are present in rapid interconversion in solution. The interchange rates between the two species observed in aqueous solution decreases to the slow exchange limit in methanol, allowing each species to be probed independently.

Introduction

Current interest in guest-host chemistry in general, and in metal ion complexation by macrocyclic ligands in particular, has instigated the synthesis of several new classes of macrocyclic ligands.[1,2] Most of these macrocycles are neutral, although some contain charged pendant ligating groups. Such ligands involve cyclic or bicyclic structures with potential ligating atoms distributed about the molecule. Numerous macrocycles are known which contain varying combinations of oxa (O), aza (N), phospha (P), and sulfa (S), ligating atoms. These macrocycles can be tailored to accommodate specific metal ions or groups of metal ions by adjusting macrocyclic cavity size and/or ligating moieties. Ligands such as crown ethers, cryptands, cavitands, and calixarines, to name a few, are of potential interest in establishing the rules for guest-host interactions.[3] Among the potential applications of complexes formed by macrocyclic ligands of this type are synthetic ionophores, NMR imaging agents, phase-transfer catalysts, ion-selective chelators, and extraction reagents.[4]

The coordination chemistry of macrocyclic ligands is most highly developed for the alkali-metal and alkaline-earth-metal ions which play important roles in biological processes.[5] Metal ions in these two groups are quite difficult to probe directly, owing to their unfavorable magnetic and spectroscopic properties. The replacement of these ions, specifically Ca^{2+} by Eu^{3+}, is well established and is possible due to the metric and chemical similarities of these two metal ions.[6,7] Eu^{3+} is a valuable structural probe due to its ability to luminesce in solution at room temperature. Furthermore, it possesses a nondegenerate ground ($^7F_0$) and first-excited ($^5D_0$) state,[8,9] neither of which can be split by the ligand field. Barring accidental coincidences, the resulting electronic transition consists of a single band for each distinct Eu^{3+} environment. The remaining energy levels of Eu^{3+} (e.g. $^5D_1$, $^5D_2$, etc.) are degenerate in the free ion and will be split into the various Stark components depending on the symmetry of the ligand field. The $^7F_0 \rightarrow {}^5D_0$ excitation profile of Eu^{3+}, which occurs in the 577-581-nm range, is obtained by scanning a tunable dye laser through the transition region while monitoring the "hypersensitive" $^5D_0 \rightarrow {}^7F_2$ emission band at 614 nm.

Amino carboxylic acids have been studied extensively because of their outstanding chelating abilities.[10] The focus of the published studies has been on noncyclic forms of these chelating agents, principally ethylenediaminetetraacetic acid (EDTA). EDTA has been the most widely studied amino carboxylate ligand since its discovery in 1935 and is known to form very stable complexes with a host of metal ions; consequently, it has the largest number of industrial and medicinal applications of any known ligand.[11] A major drawback of EDTA and other noncyclic amino carboxylates is their inability to bind to metal ions in a selective manner. Recently, a series of macrocyclic ligands containing the highly desirable amino carboxylate core were reported.[12] These macrocycles consist of the basic EDTA core in which two of the carboxylate arms are connected by varying lengths of polyether linkages (Chart I).

Chart I. Structures of Ligands 1-4[a]

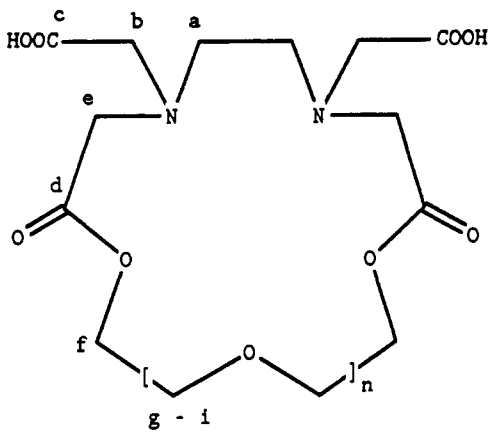

[a] Key: $n = 0$, **1**; $n = 1$, **2**; $n = 2$, **3**; $n = 3$, **4**.

Ligand protonation constants and lanthanide complex stability constants have been reported, but little is known about the structural properties of the complexes formed. In the present study, the spectroscopic characteristics of the Eu^{3+} complexes of ligands **1-4** and the open-chain analogue EDTA, for comparison purposes, are examined in aqueous and nonaqueous (methanolic) solutions. The Eu^{3+} complexation was probed by exploiting the laser-induced luminescence and excited-state lifetime spectroscopic

[†] The Pennsylvania State University.
[‡] Squibb Institute for Medical Research.

(1) Lehn, J.-M. *Acc. Chem. Res.* **1978**, *11*, 49.
(2) Christensen, J. J.; Eatough, D. J.; Izatt, R. M. *Chem. Rev.* **1973**, *74*, 351.
(3) (a) Webber, E.; Vögtle, F. *Top. Curr. Chem.* **1981**, *98*, 1. (b) Cram, D. J.; Trueblood, K. N. *Top. Curr. Chem.* **1981**, *98*, 163.
(4) (a) Blasius, E.; Janzen, K.-J. *Top. Curr. Chem.* **1981**, *98*, 163. (b) Hancock, R. D.; Martell, A. *Chem. Rev.* **1989**, *89*, 1845.
(5) Suelta, C. H. In *Metal Ions in Biological Systems*; Sigel, H., Ed.; Marcel Dekker: New York, 1974; Vol. 3, pp 201-251.
(6) Horrocks, W. DeW., Jr. *Adv. Inorg. Biochem.* **1982**, *4*, 201.
(7) Reuben, J. In *Handbook on the Physics and Chemistry of Rare Earths*; Gschneidner, K. A., Eyring, L., Eds.; North-Holland: Amsterdam, 1979; Vol. 4, pp 515-552.
(8) Horrocks, W. DeW., Jr.; Sudnick, D. R. *Acc. Chem. Res.* **1981**, *4*, 384.
(9) Horrocks, W. DeW., Jr.; Albin, M. *Prog. Inorg. Chem.* **1984**, *31*, 1.
(10) Moeller, T.; Martin, D. F.; Thompson, L. C.; Ferrus, R.; Feistel, G. R.; Randall, W. J. *Chem. Rev.* **1965**, *65*, 1.
(11) Bulman, R. A. *Struct. Bonding (Berlin)* **1987**, *67*, 91.
(12) Chang, C. A.; Chang, P. H.-L.; Qin, S.-Y. *Inorg. Chem.* **1988**, *27*, 944.

0020-1669/91/1330-3270$02.50/0

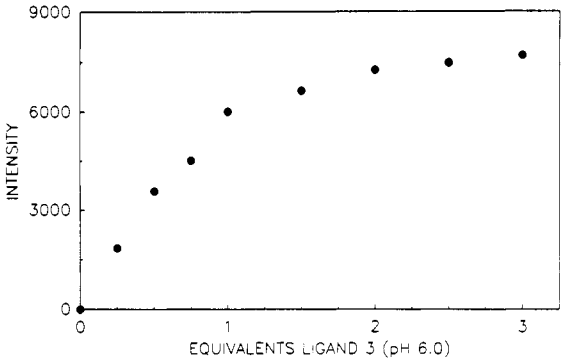

Figure 1. Amplitude of the $^7F_0 \rightarrow {}^5D_0$ excitation spectra of $[Eu(3)]^+$ (λ_{ex} = 579.6 nm; λ_{em} = 614 nm) as a function of equivalents of added ligand **3**.

techniques developed in this laboratory.[8] In aqueous solution, the structures of the Y^{3+} adducts of **1–4** and EDTA were further studied through the use of ^1H and ^{13}C NMR spectroscopy.

Experimental Section

Materials. The disodium salt of EDTA (98%), hydrated europium chloride (99.9%), methanol-d_1 (99.9%), and D_2O (99.8%) were purchased from the Aldrich Chemical Co. Piperazine hexahydrate was purchased from the Sigma Chemical Co. Spec-grade methanol was purchased from the Fisher Scientific Co. Rhodamine 590, Coumarin 485, and Coumarin 480 laser dyes were purchased from the Exciton Co., while Rhodamine 610 was obtained from the Kodak Chemical Co. The H_2O used was deionized and doubly distilled and all remaining reagents were the purest commercially available. The $EuCl_3$ stock solution used was standardized with EDTA by using an arsenazo indicator.[13] Ligands **1–4** were synthesized and fully characterized as previously reported.[12]

Methods. A Quantel series YG581C pulsed (10 Hz) Nd:YAG laser pumped tunable dye laser Model TDL50 was used as the excitation source for the luminescence experiments. The detected emission was processed by a Tracor-Northern Model TN-1505 signal averager interfaced to an IBM 9000 microcomputer. The remainder of the system was identical with that described in detail elsewhere.[14] A 10 mM stock solution (15 mM piperazine buffer, pH 6.0) was prepared for each ligand studied. The metal–ligand solutions were typically prepared in a 1:1 ratio at a concentration of 10 μM, pH 6.0, unless otherwise stated. The $^7F_0 \rightarrow {}^5D_0$ transition (580 nm) of Eu^{3+} was excited by using a mixture of Rhodamine 590 and 610 dyes, the $^7F_0 \rightarrow {}^5D_1$ transition (525 nm) was excited using a Coumarin 485 dye, and the $^7F_0 \rightarrow {}^5D_2$ transition (465 nm) was accessed with a Coumarin 480 dye. The $^5D_0 \rightarrow {}^7F_2$ emission band at 614 nm was monitored in each case. The ^1H and ^{13}C NMR spectra were recorded on a Bruker AM-300 spectrometer at 300 and 75 MHz, respectively. The ^1H and ^{13}C chemical shifts are reported relative to TMS as an external standard. NMR samples of ligands **1–4** and EDTA were prepared in a 1:1 metal:ligand ratio at concentrations of 20 and 100 mM, respectively, in D_2O at pD 6.0.

Results and Discussion

Eu^{3+} Luminescence in Aqueous Solution. The stoichiometry of these complexes was determined by titrating each ligand into an aqueous buffered 10 μM $EuCl_3$ solution at pH 6 (except for ligand **1**, which was titrated at pH 6.5). The $^7F_0 \rightarrow {}^5D_0$ excitation spectral intensities were plotted as a function of the equivalents of added ligand for each ligand studied. Such a plot is shown in Figure 1 for ligand **3**. All four of these ligands as well as EDTA exhibit similar titration curves which effectively level off at 1:1 metal:ligand ratios. These data indicate the formation of principally 1:1 complexes at the Eu^{3+} concentrations used in our experiments. The $^7F_0 \rightarrow {}^5D_0$ excitation spectra recorded at 20 °C for Eu^{3+} complexes of **1–4** consist of two well-resolved bands at 579.6 and 580.1 nm, as shown in Figure 2 for ligand **2** and EDTA. The spectra of the macrocyclic complexes are virtually identical in wavelength of peak maxima and peak height ratios with that observed for $[EuEDTA]^-$. Furthermore, they exhibit similar excited-state lifetimes. Since two isomeric species are present in solution for each ligand studied and the excited-state

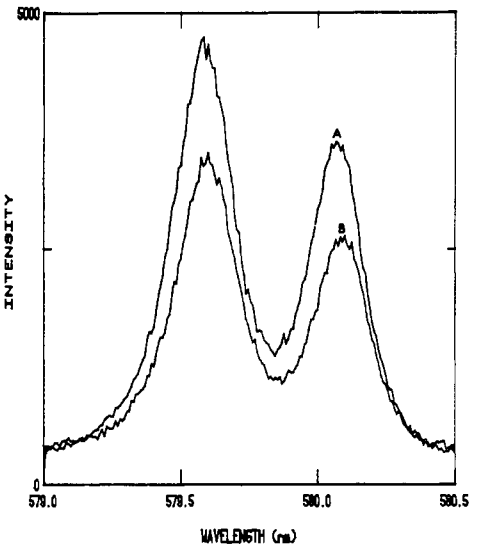

Figure 2. $^7F_0 \rightarrow {}^5D_0$ excitation spectra of (A) $[EuEDTA]^-$ and (B) $[Eu(2)]^+$.

Table I. $^7F_0 \rightarrow {}^5D_0$ Luminescence Excitation Results for the Eu^{3+} Complexes of Ligands **1–4** and EDTA in Water at 20 °C

	λ,[a] nm	E, cm^{-1}	τ_H^{-1}, ms^{-1}	τ_D^{-1}, ms^{-1}	q[b]
		$[EuEDTA]^-$			
$^7F_0 \rightarrow {}^5D_0$	579.65	17252	3.18	0.38	2.9
	580.10	17.238	3.18	0.38	2.9
		$[Eu(1)]^+$			
$^7F_0 \rightarrow {}^5D_0$	579.58	17255	3.08	0.38	2.8
	580.06	17240	3.08	0.38	2.8
		$[Eu(2)]^+$			
$^7F_0 \rightarrow {}^5D_0$	579.63	17249	3.03	0.38	2.8
	580.12	17238	3.03	0.38	2.8
		$[Eu(3)]^+$			
$^7F_0 \rightarrow {}^5D_0$	579.61	17253	3.17	0.38	2.9
	580.08	17269	3.17	0.38	2.9
		$[Eu(4)]^+$			
$^7F_0 \rightarrow {}^5D_0$	579.65	17252	3.12	0.38	2.9
	580.13	17238	3.12	0.38	2.9

[a] The reported wavelength values are accurate to ±0.02 nm. [b] Number of coordinated water molecules ± 0.5.

lifetimes are identical, it can be concluded that the interconversion rate between these two species is fast on the $^5D_0$ excited-state time scale.[15] Each of the spectra recorded were decomposed into Lorentzian–Gaussian type peaks by using a Marquardt nonlinear regression algorithm.[16] The spectral and excited-state lifetime data for all of the complexes are given in Table I.

As shown by Horrocks and Sudnick,[17] the reciprocal excited-state lifetimes, τ^{-1}, taken separately in H_2O and D_2O, may be employed to determine the number of water molecules, q, coordinated to Eu^{3+} via eq 1. Excited-state lifetimes were recorded

$$q = 1.05(\tau^{-1}_{H_2O} - \tau^{-1}_{D_2O}) \quad (1)$$

at various wavelengths across the spectral profiles of each Eu^{3+} macrocyclic complex. The observed lifetimes are independent of excitation wavelength (Table I). These lifetimes are also similar to those recorded for $[EuEDTA]^-$. The excited-state lifetime data reveal that the Eu^{3+} complexes of **1–4** and EDTA coordinate three water molecules each (Table I). The coordination of three water molecules for the Eu^{3+} complex of EDTA is in agreement with several previous studies[17-20] as well as with X-ray crystallographic

(13) Fritz, J. S.; Oliver, R. T.; Pietrzyk, D. J. *Anal. Chem.* **1958**, *30*, 1111.
(14) Tingey, J. M. Ph.D. Thesis, The Pennsylvania State University, 1987.
(15) Horrocks, W. DeW., Jr.; Arkle, V. K.; Liotta, F. J.; Sudnick, D. R. *J. Am. Chem. Soc.* **1983**, *105*, 3455.
(16) McNemar, C. W.; Horrocks, W. DeW., Jr. *Appl. Spectrosc.* **1989**, *43*, 816.
(17) Horrocks, W. DeW., Jr.; Sudnick, D. R. *J. Am. Chem. Soc.* **1979**, *101*, 334.

data for $[LnEDTA]^-$ complexes.[21,22]

The near identity of the luminescence results of ligands **1–4** and EDTA prompted us to examine the ^1H and ^{13}C NMR spectra of each of the free macrocyclic ligands and EDTA. These NMR data, recorded in D_2O solution, reveal that ligands **1–4** have the structures indicated in Chart I. The luminescence spectra and excited-state lifetime data on coordinated water molecules, taken together, suggest that the ether oxygens of the macrocyclic ring are not involved in direct coordination to the Eu^{3+} ion in aqueous solution. Crystallographic studies[23,24] have shown that when a Ln^{3+} ion is presented with a choice of coordination to a crown ether oxygen or to a water molecule, the latter is frequently chosen, with the crown ether oxygen remaining unbound. The $^7F_0 \rightarrow {}^5D_0$ excitation spectral results suggest that the ligand fields imposed on the Eu^{3+} ion by ligands **1–4** and EDTA are quite similar. These findings are further corroborated by the ligand-field splitting of the higher components of the energy level manifold (i.e. $^5D_1$, $^5D_2$). The $^7F_0 \rightarrow {}^5D_1$ and $^7F_0 \rightarrow {}^5D_2$ excitation spectra of ligands **1–4** and EDTA each contain identical numbers of bands, which appear at comparable energies (Table II). It is noteworthy that the observation of more than five $(2J + 1)$ components in the $^7F_0 \rightarrow {}^5D_2$ excitation spectra is also consistent with the presence of more than one species. An accurate determination of the metal ion site symmetry from these data is not possible, however, due to the existence of more than one species in solution. Nevertheless, the symmetry is expected to be low, likely less than C_{2v}.

These results suggest a Eu^{3+} coordination number of 8 or 9 for each of these macrocycles, depending on whether or not both carboxylate moieties coordinate. Since the potential ligating ether oxygen atoms of the macrocyclic ring appear not to bind, macrocyclic cavity size might have been expected to be a minor factor in Eu^{3+} coordination. However, the logarithmic complex formation constants of ligands **1–4** with Eu^{3+} range over 4 orders of magnitude from 10.03 to 6.06, with **3 > 4 > 2 > 1**.[12] This implies that the macrocyclic cavity size does indeed play an important role, even in the absence of ether oxygen coordination. Macrocyclic ring size and rigidity, due to the ester linkages, may affect the metal–amine or metal–carboxylate bond angles and distances and/or any hydrogen-bonding interactions between the macrocyclic ether oxygens and coordinated water molecules. While at present no X-ray crystallographic data are available for these complexes, structures of the coordinated EDTA core similar to those observed in X-ray studies of several $[Ln(EDTA)(H_2O)_3]^-$ complexes[21,22] are likely.

The importance of the macrocyclic cavity size in ligands **2–4** is further reflected in the reported complex formation constants across the lanthanide series.[12] These values are at a maximum at Eu^{3+} for ligands **2** and **3** and at Tb^{3+} for ligand **4**. On the other hand, the complex formation constants for ligand **1** increase steadily across the series from La^{3+} to Lu^{3+}, which suggests that the macrocyclic cavity of this ligand is too small to provide any selectivity among these ions. Moreover, EDTA and the *N,N'*-diethyl ester of EDTA show little selectivity across the lanthanide series; however, the latter ligand binds Eu^{3+} considerably less tightly (pK_d = 10.36) than does EDTA (pK_d = 17.99). The similarity in the Eu^{3+} complex formation constants for ligands **2–4** and the *N,N'*-diethyl ester complex of EDTA (pK_d = 8.80, 10.03, 9.89, and 10.36, respectively) suggests that the degree of hydration of the metal ion is comparable, since the binding of lanthanide ions is primarily entropy driven.[7] While the hydration number of the *N,N'*-diethyl ester is unknown, the Eu^{3+} complexes of ligands **2–4** all involve three water molecules. This information also implies that the ether oxygens of the macrocycle are not directly involved in Eu^{3+} coordination; however, the size of the macrocyclic cavity has a definite impact on the magnitude of the binding constants.

Table II. Ligand-Field Splitting of the $^5D_1$ and $^5D_2$ Levels of the Eu^{3+} Complexes of Ligands **1–4** and EDTA As Determined via Excitation Spectroscopy

	λ, nm	E, cm^{-1}
	[EuEDTA]$^-$	
$^7F_0 \rightarrow {}^5D_1$	525.43	19032
	526.00	19011
	526.32	19000
$^7F_0 \rightarrow {}^5D_2$	464.98	21506
	465.24	21494
	465.40	21487
	465.89	21464
	466.31	21445
	467.10	21409
	[Eu(**1**)]$^+$	
$^7F_0 \rightarrow {}^5D_1$	525.28	19038
	525.84	19017
	526.33	19000
$^7F_0 \rightarrow {}^5D_2$	464.89	21511
	465.25	21494
	465.43	21486
	465.90	21464
	466.33	21444
	467.13	21407
	[Eu(**2**)]$^+$	
$^7F_0 \rightarrow {}^5D_1$	525.41	19033
	525.99	19012
	526.33	19000
$^7F_0 \rightarrow {}^5D_2$	464.90	21510
	465.23	21495
	465.41	21486
	465.89	21464
	466.33	21444
	467.13	21407
	[Eu(**3**)]$^+$	
$^7F_0 \rightarrow {}^5D_1$	525.44	19032
	525.99	19012
	526.33	19000
$^7F_0 \rightarrow {}^5D_2$	464.89	21511
	465.22	21495
	465.37	21488
	465.88	21465
	466.36	21443
	467.13	21407
	[Eu(**4**)]$^+$	
$^7F_0 \rightarrow {}^5D_1$	525.44	19032
	526.00	19011
	526.33	19000
$^7F_0 \rightarrow {}^5D_2$	464.80	21515
	465.20	21496
	465.42	21486
	465.86	21466
	466.34	21444
	467.13	21407

NMR Studies. The proposed solution structures of these lanthanide macrocyclic complexes are further supported by ^1H and ^{13}C NMR data on the Y^{3+} adducts. Y^{3+} was chosen as the replacement ion for Eu^{3+} in these NMR studies due to its similar ionic radius, chemical behavior, and diamagnetic character. The ^1H and ^{13}C chemical shift data for the Y^{3+} adducts are reported in Tables III and IV. The ^1H data indicate that the acetate protons (b) and the methylene ester protons (e) become indistinguishable upon metal binding. These protons exhibit an AB splitting pattern indicative of long-lived metal–nitrogen bonds and short-lived metal–oxygen bonds on the NMR time scale.[25,26] An

(18) Bryden, C. C.; Reilley, C. N. *Anal. Chem.* **1982**, *54*, 610.
(19) Halwani, J.; Dexpert-Ghys, J.; Piriou, B.; Caro, P. *Analusis* **1987**, *15*, 299.
(20) Dexpert-Ghys, J.; Halwani, J.; Piriou, B. *Inorg. Chim. Acta* **1987**, *139*, 303.
(21) Hoard, J. L.; Lee, B.; Lind, M. D. *J. Am. Chem. Soc.* **1965**, *87*, 1612.
(22) Nassimbeni, L. R.; Wright, M. R. W.; van Niekerk, J. C.; McCallum, P. A. *Acta Crystallogr.* **1979**, *B35*, 1341.
(23) Parvez, M.; Breen, P. J.; Horrocks, W. DeW., Jr. *Lanthanide Actinide Res.* **1988**, *2*, 153.
(24) Bunzli, J.-C. G.; Wessner, D. *Isr. J. Chem.* **1984**, *24*, 313.
(25) Day, R. J.; Reilley, C. N. *Anal. Chem.* **1964**, *36*, 1073.

Table III. ^{1}H NMR Data of the Free Ligands **1–4** and Their Y^{3+} Complexes in D_2O Solution at 20 °C

	EDTA	
a	NCH_2CH_2	3.45 (s, 4)
b	NCH_2COOH	3.76 (s, 8)
	Ligand **1**	
a	NCH_2CH_2	3.21 (s, 4)
b	NCH_2COOH	3.85 (s, 4)
e	NCH_2COOCH_2	3.57 (s, 4)
f	$COOCH_2CH_2$	4.51 (s, 4)
	Ligand **2**	
a	NCH_2CH_2	3.27 (s, 4)
b	NCH_2COOH	3.98 (s, 4)
e	NCH_2COOCH_2	3.74 (s, 4)
f	$COOCH_2CH_2$	4.36 (m, 4)
g	$COOCH_2CH_2O$	3.72 (m, 4)
	Ligand **3**	
a	NCH_2CH_2	3.27 (s, 4)
b	NCH_2COOH	4.02 (s, 4)
e	NCH_2COOCH_2	3.75 (s, 4)
f	$COOCH_2CH_2$	4.35 (m, 4)
g	$COOCH_2CH_2O$	3.71 (m, 4)
h	OCH_2CH_2O	3.62 (s, 4)
	Ligand **4**	
a	NCH_2CH_2	3.26 (s, 4)
b	NCH_2COOH	3.98 (s, 4)
e	NCH_2COOCH_2	3.77 (s, 4)
f	$COOCH_2CH_2$	4.32 (m, 4)
g	$COOCH_2CH_2O$	3.74 (m, 4)
h, i	OCH_2CH_2O	3.63 (m, 8)
	$[Y(EDTA)]^-$	
a	NCH_2CH_2	2.86 (s, 4)
b	NCH_2COOH	3.58, 3.52, 3.37, 3.31 (AB, 8)
	$[Y(1)]^+$	
a	NCH_2CH_2	2.78 (s, 4)
b, e	NCH_2COOH, NCH_2COOCH_2	3.49, 3.44, 3.27, 3.22 (AB, 8)
f	$COOCH_2CH_2$	3.60 (s, 4)
	$[Y(2)]^+$	
a	NCH_2CH_2	2.78 (s, 4)
b, e	NCH_2COOH, NCH_2COOCH_2	3.49, 3.44, 3.28, 3.22 (AB, 8)
f	$COOCH_2CH_2$	3.68 (m, 4)
g	$COOCH_2CH_2O$	3.58 (m, 4)
	$[Y(3)]^+$	
a	NCH_2CH_2	2.77 (s, 4)
b, e	NCH_2COOH, NCH_2COOCH_2	3.49, 3.43, 3.27, 3.21 (AB, 8)
f	$COOCH_2CH_2$	3.67 (m, 4)
g	$COOCH_2CH_2O$	3.59 (m, 4)
h	OCH_2CH_2O	3.65 (s, 4)
	$[Y(4)]^+$	
a	NCH_2CH_2	2.77 (s, 4)
b, e	NCH_2COOH, NCH_2COOCH_2	3.48, 3.43, 3.27, 3.21 (AB, 8)
f	$COOCH_2CH_2$	3.66 (M, 4)
g	$COOCH_2CH_2O$	3.57 (m, 4)
h, i	OCH_2CH_2O	3.64 (s, 8)

AB splitting pattern is also observed for $[YEDTA]^-$ at 20 °C, in excellent agreement with the previously reported spectrum,[27] except that the resonances of the AB quartet are shifted slightly downfield from those of ligands **1–4**. The proton resonances of the ethylenic groups connecting the ether oxygens are virtually unaffected by metal complexation, as would be expected if the ether oxygens are not involved in direct coordination to the metal ion. The ^{13}C data further establish that the carboxylate methylene carbon atoms (c) and the ester methylene carbon atoms (d) become equivalent upon metal complexation. The acetate carbons (b) and the methylene ester carbons (e) also become equivalent upon Y^{3+} complexation. Two distinct carboxylate carbon (c)

Table IV. ^{13}C NMR Data of the Free Ligands **1–4** and Their Y^{3+} Complexes in D_2O Solution at 20 °C

	EDTA	
a	NCH_2CH_2	51.74
b	NCH_2COOH	58.19
c	NCH_2COOH	170.80
	Ligand **1**	
a	NCH_2CH_2	52.40
b	NCH_2COOH	58.47
c	NCH_2COOH	169.86
d	$NCH_2COOCH2$	174.05
e	NCH_2COOCH_2	56.86
f	$COOCH_2CH_2$	62.49
	Ligand **2**	
a	NCH_2CH_2	51.76
b	NCH_2COOH	56.52
c	NCH_2COOH	170.01
d	$NCH_2COOCH2$	172.44
e	NCH_2COOCH_3	54.87
f	$COOCH_2CH_2$	64.16
g	$COOCH_2CH_2O$	68.13
	Ligand **3**	
a	NCH_2CH_2	51.79
b	NCH_2COOH	56.54
c	NCH_2COOH	169.98
d	$NCH_2COOCH2$	172.43
e	NCH_2COOCH_2	55.00
f	$COOCH_2CH_2$	64.99
g	$COOCH_2CH_2O$	68.60
h	OCH_2CH_2O	69.93
	Ligand **4**	
a	NCH_2CH_2	51.22
b	NCH_2COOH	56.21
c	NCH_2COOH	170.15
d	$NCH_2COOCH2$	172.73
e	NCH_2COOCH_2	54.66
f	$COOCH_2CH_2$	65.15
g	$COOCH_2CH_2O$	68.40
h	OCH_2CH_2O	69.90
i	OCH_2CH_2O	70.07
	$[Y(EDTA)]^-$	
a	NCH_2CH_2	58.17
b	NCH_2COOH	63.25
c	NCH_2COOH	180.19
	$[Y(1)]^+$	
a	NCH_2CH_2	58.12
b	NCH_2COOH	63.11
c, d	NCH_2COOR	180.10
f	$COOCH_2CH_2$	62.68
	$[Y(2)]^+$	
a	NCH_2CH_2	58.11
b, e	NCH_2COOR	63.09
c, d	NCH_2COOR	180.09
d	$COOCH_2CH_2$	60.57
e	$COOCH_2CH_2O$	71.73
	$[Y(3)]^+$	
a	NCH_2CH_2	58.11
b, e	NCH_2COOR	63.08
c, d	NCH_2COOR	180.09
f	$COOCH_2CH_2$	60.49
g	$COOCH_2CH_2O$	71.83
h	OCH_2CH_2O	69.66
	$[Y(4)]^+$	
a	NCH_2CH_2	58.15
b, e	NCH_2COOR	63.14
c, d	NCH_2COOR	180.11
f	$COOCH_2CH_2$	60.55
g[a]	$COOCH_2CH_2O$	71.88
h	OCH_2CH_2O	69.63
i	OCH_2CH_2O	69.84

[a] R = CH_2 or H.

(26) Day, R. J.; Reilley, C. N. *Anal. Chem.* **1965**, *37*, 1326.
(27) Baisden, P. A.; Choppin, G. R.; Garrett, B. B. *Inorg. Chem.* **1977**, *16*, 1367.

Chart II. Schematic Representation of the Possible Solution Structures of the Eu^{3+} Complexes of Ligands **1–4**.

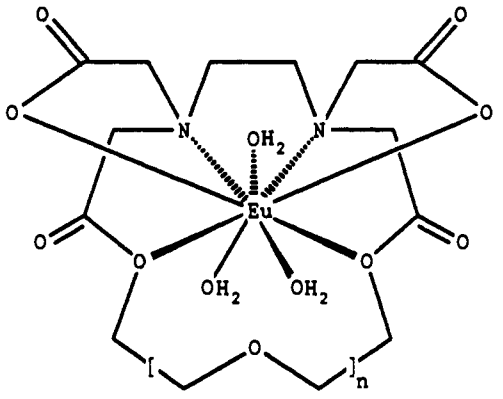

resonances are observed at approximately 170 and 173 ppm for the free ligands **1–4** but only a single sharp resonance at approximately 180 ppm is observed for the Y^{3+} complexes. The deshielding and indistinguishable nature of these nuclei are caused by metal binding. This result is consistent with the direct coordination of the acetate and ester moieties, which render their chemical environments similar. Upon complex formation, the chemical shifts of the ethylenic carbons (h and i) of the ether linkages remain virtually unchanged from their free ligand values, additionally substantiating the idea that the ether moieties do not coordinate to the metal ion.

These luminescence and NMR data clearly demonstrate the nonbonding character of the ether oxygens and the indistinguishable nature of the acetate and ester functionalities. The ligand field imposed upon the metal ion by each of these macrocycles is thus virtually identical with that of EDTA. These results are consistent with the coordination of both amine nitrogen atoms, both ester moieties, and one or two carboxylate groups of the macrocyclic ligands, and three water molecules (Chart II). This provides the metal ion with a coordination number of 8 or 9 depending on whether or not both carboxylate groups coordinate. Hence, the only differences in the ligating moieties between the macrocyclic ligands **1–4** and EDTA is that, in the former, two of the carboxylate moieties of the EDTA core are constrained in a particular binding configuration via ester formation and, of course, the overall charge of the macrocyclic complexes is decreased by two. It follows that the two species observed in the Eu^{3+} $^7F_0 \rightarrow {}^5D_0$ excitation spectrum of all of these complexes are due to a rapid exchange between bound and unbound carboxylate groups, as previously suggested.[28] This exchange process might be expected to be temperature and/or pH dependent, prompting a study of the $^7F_0 \rightarrow {}^5D_0$ excitation spectra of these complexes as a function of both variables.

Temperature Studies. Each Eu^{3+} complex was studied over the temperature range 10–90 °C. As the temperature increases, the relative intensities of the excitation bands become reversed. At the highest temperature (90 °C), the longer wavelength band is more than twice as intense as the shorter wavelength band. Similar results were previously reported for $[EuEDTA]^-$ in which an absorption spectral equilibrium shift was interpreted as the loss of a bound water molecule.[29] The excited-state lifetimes, recorded at each temperature and at various wavelengths across the spectral profile for each Eu^{3+} complex, remain constant at all temperatures studied. These data suggest that the equilibrium between the two observed species does not involve a change in the number of coordinated water molecules. Similar results were obtained for EDTA. This temperature-dependent equilibrium is postulated to be an interconversion between species with a bound and an unbound carboxylate moiety with a concomitant change in total coordination number, rather than in the number of water molecules.

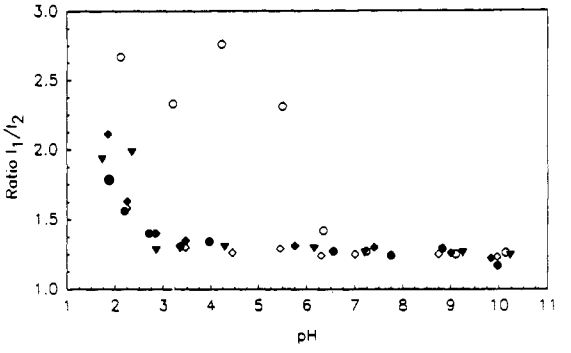

Figure 3. Ratio of the 579.6 (I_1) and 580.1 (I_2) nm bands of ligands **1** (○), **2** (●), **3** (◇), **4** (◆), and EDTA (▼) as a function of pH.

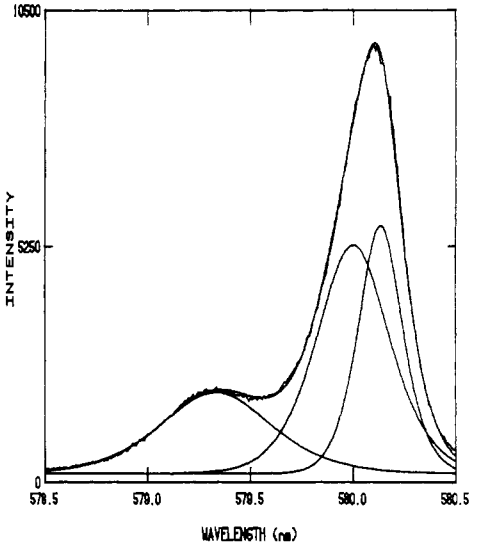

Figure 4. Deconvoluted $^7F_0 \rightarrow {}^5D_0$ excitation spectrum of $[Eu(4)]^+$ in methanol using Lorentzian–Gaussian type peaks.

pH Studies. As the pH is increased from 2 to 10 the $^7F_0 \rightarrow {}^5D_0$ excitation spectral peak wavelengths of ligands **1–4** and EDTA remain unchanged, but the ratio of the intensities of the two bands is affected (Figure 3). For ligands **2–4** and EDTA the shorter wavelength band has nearly twice the intensity of the longer wavelength band at a pH value of 2. This ratio decreases with increasing pH until pH 3.5, beyond which the ratio remains constant at 1.3, through pH 10. Representative $^7F_0 \rightarrow {}^5D_0$ excitation spectra of two of these complexes at pH values greater than 3.5 are shown in Figure 2. The intensities of the two bands observed for ligand **1** differ from those of the other macrocyclic Eu^{3+} complexes. The intensity of the shorter wavelength band remains approximately twice that of the longer wavelength band until pH values of ~5.5 are reached. Above this pH value the intensity of the longer wavelength band increases until it is two-thirds that of the shorter wavelength band and identical with that of complexes of ligands **2–4** and EDTA. The excited-state lifetimes for each of the Eu^{3+} complexes increases slightly from approximately 315 μs in the pH range 3.5–7.5 to 360 μs at pH values greater than 8.0. This increase is attributed to the onset of the deprotonation of a bound water molecule at higher pH values.

Eu^{3+} Complexation in Methanol. Studies of these complexes in the more weakly coordinating solvent methanol (MeOH) were undertaken in an attempt to achieve coordination of the ether oxygens of the macrocyclic ring. The $^7F_0 \rightarrow {}^5D_0$ excitation spectra of the 1:1 Eu^{3+} complexes of ligands **1–4** and EDTA are dramatically altered from those observed in water (compare Figures 2 and 4). Superficially, each spectrum appears to consist of two bands with the asymmetric longer wavelength band being dominant. However, using our well-tested Marquardt algorithm-based

(28) Sudnick, D. R. Ph.D. Thesis, The Pennsylvania State University, 1979.
(29) Geier, G.; Jorgensen, C. K. *Chem. Phys. Lett.* **1971**, *9*, 263.

Table V. $^7F_0 \rightarrow {}^5D_0$ Luminescence Excitation Results for the Eu^{3+} Complexes of Ligands **1–4** and EDTA in Methanol at 20 °C

	λ,[a] nm	E, cm^{-1}	τ_H^{-1}, ms^{-1}	τ_D^{-1}, ms^{-1}	m[b]
		[EuEDTA]$^-$			
$^7F_0 \rightarrow {}^5D_0$	579.39	17260	1.76	0.45	2.7
	579.98	17242	1.39	0.45	2.0
	580.14	17237	0.84	0.45	0.8
		[Eu(**1**)]$^+$			
$^7F_0 \rightarrow {}^5D_0$	579.34	17261	1.85	0.56	2.9
	579.95	17243	1.53	0.48	2.1
	580.15	17237	1.53	0.48	2.1
		[Eu(**2**)]$^+$			
$^7F_0 \rightarrow {}^5D_0$	579.35	17261	1.94	0.54	2.9
	579.97	17242	1.46	0.54	2.1
	580.14	17237	1.46	0.48	2.1
		[Eu(**3**)]$^+$			
$^7F_0 \rightarrow {}^5D_0$	579.37	17260	1.87	0.54	2.8
	579.98	17242	1.50	0.48	2.1
	580.09	17239	1.50	0.48	2.1
		[Eu(**4**)]$^+$			
$^7F_0 \rightarrow {}^5D_0$	579.35	17261	2.08	0.53	3.3
	579.96	17243	1.49	0.47	2.1
	580.10	17238	1.49	0.47	2.1
		$EuCl_3$ in Methanol			
$^7F_0 \rightarrow {}^5D_0$	578.87	17275	4.08	0.69	7.1

[a] The reported excitation wavelength values are accurate to ±0.02 nm. [b] Number of coordinated methanol moelcules ± 0.5.

curve-fitting procedure,[16] we observed that each spectrum clearly consists of three Lorentzian–Gaussian type peaks. A two-peak fit to these spectra is rejected on the basis of Hamilton's R factor test[30] at a confidence level of better then 99.9%. The $^7F_0 \rightarrow {}^5D_0$ excitation spectrum of [Eu(**4**)]$^+$ is presented in Figure 4 and the spectral data for each of the complexes in methanol solution are given in Table V. Using the stability constant reported[31] for the formation of the $LaCl^{2+}$ complex in methanol solution, we estimate that even in the absence of added macrocyclic ligand, less than 5% of the lanthanide ion will be complexed by chloride under the conditions of our experiment. Hence none of the observed spectral features can be attributed to chloride complexation.

The luminescence decay curves recorded for complexes of ligands **1–4** in methanol at several wavelengths across the spectral profile were resolved into their respective components. Two excited-state lifetime components were observed in the central regions of the spectral profiles, while only a single lifetime component was obtained at either end of each spectrum (Table V). The shorter lifetime is the major component at shorter wavelengths while the longer component dominates at longer wavelengths. Three exponential components were resolved from the luminescence decay curve of EDTA in methanol. The shortest component was only detectable at shorter wavelengths while the intermediate and longest lifetimes are both present at longer wavelengths. From the relative amplitudes of the two lifetime components taken across the asymmetric peak profiles of the macrocyclic ligand complexes, assignments of the respective lifetimes to the curve-resolved bands were made (Table V). These results (three peaks, two lifetimes) indicate the presence of two species in fast exchange and a third species in slow exchange with the first two, on the $^5D_0$ excited-state time scale for complexes of ligands **1–4**. In contrast, the EDTA system exhibits three species all in slow exchange with one another.

Excited-state lifetime data were recorded in methanol-d_1 (MeOD) in order to determine the number of coordinated methanol moieties. Luminescence decay curves were recorded across the spectral profile for each Eu^{3+} complex of ligands **1–4** and EDTA. The equation used to determine m, the number of bound methanol molecules, is

$$m = 2.1(\tau^{-1}_{MeOH} - \tau^{-1}_{MeOD}) \quad (2)$$

where τ^{-1} is the reciprocal excited-state lifetime, taken separately in MeOH and MeOD. This equation is based on the well-known method[17] of determining the number of coordinated water molecules bound to Eu^{3+} and Tb^{3+} ions through the replacement of O–H oscillators by O–D oscillators. For MeOH, the assumption is that it behaves like half a water molecule since it contains only a single O–H oscillator. While no crystallographic data are available concerning the coordination of methanol moieties to Eu^{3+}, eq 2 provides a reasonable number of bound MeOH's for the free Eu^{3+} ion of 7.1 ± 0.5. The number of MeOH molecules coordinated to each of the species observed in the luminescence spectrum of [EuEDTA]$^-$ are 3, 2, and 1 ± 0.5 from lower to higher wavelengths, respectively. The Eu^{3+} complexes of ligands **1–4** in MeOH bind 3 and 2 ± 0.5 MeOH molecules, for the species with excitation maxima at lower and higher wavelengths, respectively.

These data indicate that even the more weakly coordinating solvent MeOH competes strongly with the ether oxygen potential ligating moieties of the macrocyclic ring. Nevertheless, methanol causes the exchange rates between the species present to be slowed significantly on the $^5D_0$ time scale compared to the situation in water. Our data indicate that the number of bound methanol moieties is less for the longer wavelength species. This is consistent with the loss of a neutral solvent ligand being accompanied by the coordination of a negatively charged carboxylate moiety resulting in a shift in the $^7F_0 \rightarrow {}^5D_0$ transition to longer wavelengths.[32]

Acknowledgment. This research was supported through Grant CHEM-8821707 from the National Science Foundation. We thank Drs. Patrick J. Breen and Charles W. McNemar for writing portions of the computer software used in this research.

(30) Hamilton, W. C. *Acta Crystallogr.* **1965**, *18*, 502.
(31) Bünzli, J.-C. G.; Merbach, A. E.; Nielson, R. M. *Inorg. Chim. Acta* **1987**, *139*, 151.
(32) Albin, M.; Horrocks, W. DeW., Jr. *Inorg. Chem.* **1985**, *24*, 885.